

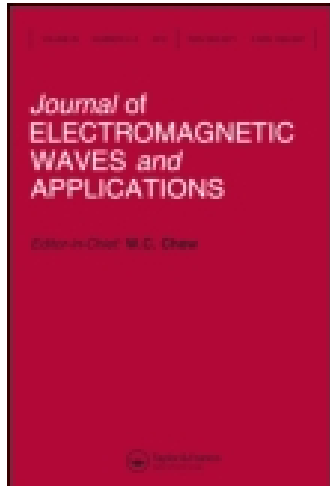
This article was downloaded by: [University of Auckland Library]

On: 14 February 2015, At: 08:37

Publisher: Taylor & Francis

Informa Ltd Registered in England and Wales Registered Number: 1072954

Registered office: Mortimer House, 37-41 Mortimer Street, London W1T 3JH,  
UK



## Journal of Electromagnetic Waves and Applications

Publication details, including instructions for authors  
and subscription information:

<http://www.tandfonline.com/loi/tewa20>

### Computer Simulation of Wave Scattering from a Dielectric Random Surface in Two Dimensions-Cylindrical Case

M.F. Chen <sup>a</sup> & S.Y. Bai <sup>b</sup>

<sup>a</sup> Wave Scattering Research Center EE Department  
University of Texas at Arlington UTA Box 19106  
Arlington, TX 76019, USA

<sup>b</sup> Wave Scattering Research Center EE Department  
University of Texas at Arlington UTA Box 19106  
Arlington, TX 76019, USA

Published online: 03 Apr 2012.

To cite this article: M.F. Chen & S.Y. Bai (1990) Computer Simulation of Wave Scattering from a Dielectric Random Surface in Two Dimensions-Cylindrical Case, *Journal of Electromagnetic Waves and Applications*, 4:10, 963-982, DOI: [10.1163/156939390X00708](https://doi.org/10.1163/156939390X00708)

To link to this article: <http://dx.doi.org/10.1163/156939390X00708>

PLEASE SCROLL DOWN FOR ARTICLE

Taylor & Francis makes every effort to ensure the accuracy of all the information (the "Content") contained in the publications on our platform. However, Taylor & Francis, our agents, and our licensors make no representations or warranties whatsoever as to the accuracy, completeness, or suitability for any purpose of the Content. Any opinions and views expressed in this publication are the opinions and views of the authors, and are not the views of or endorsed by Taylor & Francis. The accuracy of the Content should not be relied upon and should be independently verified with primary sources of information. Taylor and Francis shall not be liable for any losses, actions, claims, proceedings, demands, costs, expenses, damages, and other liabilities whatsoever or howsoever caused arising directly or indirectly in connection with, in relation to or arising out of the use of the Content.

This article may be used for research, teaching, and private study purposes.  
Any substantial or systematic reproduction, redistribution, reselling, loan, sub-  
licensing, systematic supply, or distribution in any form to anyone is expressly  
forbidden. Terms & Conditions of access and use can be found at [http://  
www.tandfonline.com/page/terms-and-conditions](http://www.tandfonline.com/page/terms-and-conditions)

## Computer Simulation of Wave Scattering from a Dielectric Random Surface in Two Dimensions—Cylindrical Case

M. F. Chen and S. Y. Bai

Wave Scattering Research Center  
EE Department  
University of Texas at Arlington  
UTA Box 19106  
Arlington, TX 76019, USA

**Abstract**—The detailed moment method simulation of wave scattering from a computer generated dielectric rough surface in two-dimensional space is given. The validity of the numerical algorithm is verified by comparing simulation results with Kirchhoff and first order small perturbation theory at their valid regions. The efficiency and versatility of the numerical simulation algorithm as a practical tool to study rough surface scattering is demonstrated. It is found that the Kirchhoff series solution always gives an estimate that is between the VV and HH polarizations for both Gaussian and composite surface if the correct correlation function is used. It is also found that for a single scale surface, the effect of increasing frequency on the backscattering coefficient is to gradually diminish the VV and HH polarization separation from that of Perturbation to Kirchhoff. For surfaces with distinctively different roughness scales, the frequency behavior of the backscattering coefficient depends on the dominance of individual scales at their respective angular range, i.e., large scale dominates at smaller angle of incidence while small scale dominates at large angle of incidence. In all cases, the effect of increasing dielectric constant is to increase the level of the scattering coefficient and the separation between VV and HH polarizations.

### I. INTRODUCTION

The problem of solving electromagnetic wave scattering from randomly rough surfaces has a long history and can be dated back as early as the 1950's [1-3]. Since then, numerous theoretical models have been developed and applied to practical problems such as the scattering from sea and terrain. Among the various theories, the most well-known ones are the small perturbation method, Kirchhoff approximation (tangent plane approximation) and geometric optics. The validity of each method depends on the approximations made pertaining to the physical conditions such as the surface roughness and frequency. For surfaces with roughness scale large compared to the wavelength, the method of Kirchhoff approximation is used. For surfaces with roughness scale small compared to the wavelength, the method of small perturbation is used. In either case, additional assumptions must be made to obtain mathematically tractable solutions. Under the Kirchhoff method, a stationary phase approximation allows an analytic solution to be derived in the form of an infinite series or by taking a further approximation of large  $k\sigma$  to reduce the expression to that of the geometric optics solution [4]. Under the small perturbation method, both the amplitude and the phase of the incident

and scattered fields are expressed in a perturbation series in terms of the small surface height. The unknown perturbation series coefficients of the scattered field amplitude can be obtained by matching the field quantities on the boundary. The mathematics involved becomes too complicated as the order of the perturbation series increases. For like polarization scattering, the usual approximation is to retain only the first order of the perturbation series. Second order is required for cross polarization scattering. For geometric optics, it can be shown that the scattering depends simply on the surface slope distribution [5]. In recent years, a few new approaches to the surface scattering problem have emerged. The integral equation model [6] seeks a correction term to the surface current in addition to the Kirchhoff approximation. The phase perturbation method [7] perturbs only the field amplitude. The intention of these recent refinements of Kirchhoff and small perturbation methods are to extend the applicability of models into the intermediate frequency range.

The verification of theories requires experimental measurements of surface scattering coefficients under controlled laboratory conditions or out in the field. To obtain complete quantitative verification of all the physical parameters involved in a theory is not practical. The method of computer simulation offers an efficient alternative. Axline and Fung [8] simulated the wave scattering from a perfectly conducting random surface by calculating the surface current density induced by an impinging plane wave by the method of moments. The scattering coefficient is obtained by averaging scattered fields from samples of computer generated random surfaces. In a later paper by Fung and Chen [9], the method of generating random profiles with specified correlation functions was developed, giving the simulation technique additional control over the statistical properties of the rough surface target. The simulation technique was also used to investigate the region of validity of the scattering theories mentioned earlier for surfaces with Gaussian and non-Gaussian statistics [10,11]. In acoustics, the same technique was also used to investigate the validity of Kirchhoff theory and the full wave method for rough surface scattering [12,13].

As we mentioned earlier, the simulation of electromagnetic wave scattering from a rough surface using the method of moments is only available for a perfectly conducting surface in two dimensional space. It is the purpose of this paper to extend the simulation technique to include scattering from dielectric surfaces so that the technique can be used as a practical tool to investigate rough surface scattering phenomenon. In Section II, the formulation of the problem along with the employment of the moment method to convert the integral equations to a matrix equation is given. The verification of the numerical algorithm by comparing simulation with theories for surfaces whose roughness conditions meet the assumption of the theories is given in Section III. Simulation results and discussions are given in Section IV. Concluding remarks are given in Section V.

## II. FORMULATION

By applying the second Green's vector identity to a closed volume, the governing surface electric field integral equation and the surface magnetic field integral equation in medium 1 (the air) can be written as [14].

$$\hat{n} \times \bar{E}^i(\bar{r}) = -\frac{1}{2}\bar{K}_s + \hat{n} \times \int_s \left[ j\omega\mu_0\phi_1\bar{J}_s - \bar{K}_s \times \nabla\phi_1 - \frac{\nabla'_s \cdot \bar{J}_s}{j\omega\epsilon_1} \nabla\phi_1 \right] ds' \quad (1a)$$

$$\hat{n} \times \bar{H}^i(\bar{r}) = \frac{1}{2}\bar{J}_s + \hat{n} \times \int_s \left[ j\omega\epsilon_1\phi_1\bar{K}_s + \bar{J}_s \times \nabla\phi_1 - \frac{\nabla'_s \cdot \bar{K}_s}{j\omega\mu_0} \nabla\phi_1 \right] ds' \quad (1b)$$

The surface integral equations in medium 2 (the surface medium) can be written as

$$0 = -\frac{1}{2}\bar{K}_s - \hat{n} \times \int_s \left[ j\omega\mu_0\phi_2\bar{J}_s - \bar{K}_s \times \nabla\phi_2 - \frac{\nabla'_s \cdot \bar{J}_s}{j\omega\epsilon_2} \nabla\phi_2 \right] ds' \quad (2a)$$

$$0 = \frac{1}{2}\bar{J}_s - \hat{n} \times \int_s \left[ j\omega\epsilon_0\phi_2\bar{K}_s - \bar{J}_s \times \nabla\phi_2 - \frac{\nabla'_s \cdot \bar{K}_s}{j\omega\epsilon_2} \nabla\phi_2 \right] ds' \quad (2b)$$

where  $\hat{n}$  is the unit outward normal to the surface,  $\bar{K}_s = -\hat{n} \times \bar{E}$ , the equivalent surface magnetic current density,  $\bar{J}_s = \hat{n} \times \bar{H}$ , the equivalent surface electric current density.

Since the problem of rough surface scattering in three-dimensional space exceeds the hardware capacity of currently available computers, in this paper only the simulation of rough surface scattering in two-dimensional space (surface variation along  $x$ - and  $z$ -axes only) is formulated. The corresponding Green's function in cylindrical coordinates is the zeroth order Hankel function of the second kind

$$\phi_i = -\frac{j}{4} H_0^{(2)}(k_i|\bar{p} - \bar{p}'|), \quad i = 1, 2$$

By applying the method of moments, the surface integral equations can be converted into system of linear equations with complex coefficients. The derivation of this conversion for both VV and HH polarizations are given in the following.

### HH polarization

Consider the scattering geometry shown in Fig. 1. For horizontally polarized incident fields of the form

$$\bar{E}^i = -\hat{y} e^{jk_1(x \sin \theta + z \cos \theta)} \quad (3a)$$

$$\bar{H}^i = \frac{1}{\eta}(-\hat{x} \cos \theta + \hat{z} \sin \theta) e^{jk_1(x \sin \theta + z \cos \theta)} \quad (3b)$$

the induced electric surface current density on the surface is only a function of the surface contour variable  $l'$ , i.e.,

$$\bar{J}_s = \hat{y} J_s(l') \quad (4)$$

Therefore

$$\nabla'_s \cdot \bar{J}_s = \frac{\partial}{\partial l'} 0 + \frac{\partial}{\partial y} J_s(l') + \frac{\partial}{\partial n'} 0 = 0 \quad (5)$$

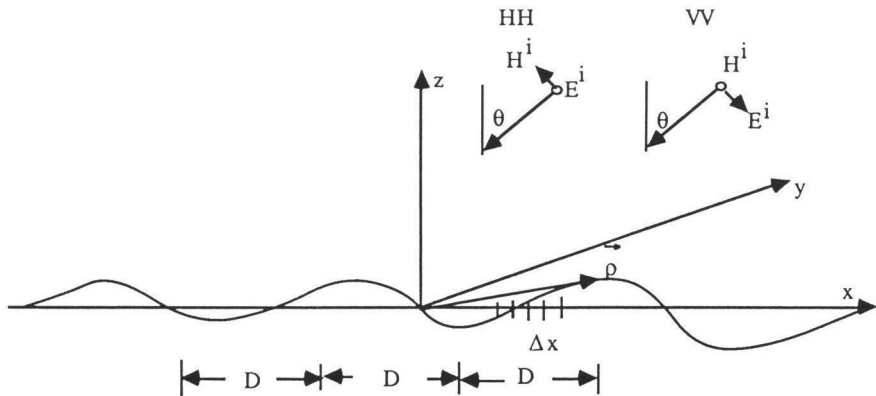


**Figure 1.** The geometry of rough surface scattering in two-dimensional space. and the pair of electric surface field integral equations (1a) and (2a) can be further reduced to

$$\hat{n} \times \bar{E}^i(\bar{\rho}) = -\frac{1}{2} \bar{K}_s + \hat{n} \times \int_s [j\omega\mu_0\phi_1 \bar{J}_s - \bar{K}_s \times \nabla\phi_1] dl' \quad (6a)$$

$$0 = -\frac{1}{2} \bar{K}_s - \hat{n} \times \int_c [j\omega\mu_0\phi_2 \bar{J}_s - \bar{K}_s \times \nabla\phi_2] dl' \quad (6b)$$

Consider the vector identity

$$\bar{K}_s \times \nabla\phi_1 = (-\hat{n}' \times \bar{E}) \times \nabla\phi_1 = -\bar{E} (\hat{n}' \cdot \nabla\phi_1), \quad i = 1, 2 \quad (7)$$

Equation (6) can be simplified to

$$E_y^i(\bar{\rho}) = \frac{1}{2} E_y(\bar{\rho}) + \int_c [j\omega\mu_0\phi_1 J_y + E_y(\hat{n}' \cdot \nabla\phi_1)] dl' \quad (8a)$$

$$0 = \frac{1}{2} E_y(\bar{\rho}) - \int_c [j\omega\mu_0\phi_2 J_y + E_y(\hat{n}' \cdot \nabla\phi_2)] dl' \quad (8b)$$

By adopting the pulse base function and using the point matching method, the above two equations can be converted into a matrix equation,

$$\begin{bmatrix} Z^{11} & Z^{12} \\ Z^{21} & Z^{22} \end{bmatrix} \begin{bmatrix} E_y \\ J_y \end{bmatrix} = \begin{bmatrix} E_y^i \\ 0 \end{bmatrix} \quad (9)$$

where the size of the matrix is  $2N \times 2N$ , with  $N$  the number of pulses used to expand the unknown current density  $J_y$  and the unknown surface field  $E_y$  over the entire illuminated surface contour. The matrix elements can be written as

$$Z_{mn}^{11} = \frac{1}{2} \delta_{mn} + \int_{\Delta l_n} (\hat{n}' \cdot \nabla\phi_1) \approx \begin{cases} \frac{1}{2} - \frac{D_n \Delta x_n}{4\pi R_c}, & m = n \\ (\hat{n}_n \cdot \hat{R}) \frac{j k_1}{4} H_1^{(2)}(k_1 |\bar{\rho}_m - \bar{\rho}_n|) D_n \Delta x_n, & m \neq n \end{cases} \quad (10)$$

Note that indices  $m, n$  are within the range  $1 < m, n < N$ .

$D_n = \sqrt{1 + (dz/dx)_n^2}$ ,  $\hat{R} = (\bar{\rho}_m - \bar{\rho}_n)/|\bar{\rho}_m - \bar{\rho}_n|$ , with  $\bar{\rho}_m$  and  $\bar{\rho}_n$  representing position vectors from the origin to surface points at  $x_m$  and  $x_n$  respectively.  $R_c$  is the radius of curvature at each point on the surface.

$$Z_{mn}^{12} = j\omega\mu_0 \int_{\Delta l_n} \phi_1 dl' \\ \approx j\omega\mu_0 \begin{cases} -\frac{j}{4} \left( 1 - \frac{2j}{\pi} \ln \frac{\gamma k_1 D_n \Delta x}{4e} \right), & m = n \\ -\frac{j}{4} H_0^{(2)}(k_1 |\rho_m - \rho_n|) D_n \Delta x, & m \neq n \end{cases} \quad (11)$$

where  $\gamma = 0.5772$  = Euler's constant.

$$Z_{mn}^{21} = \frac{1}{2} \delta_{mn} - \int_{\Delta l_n} (\hat{n}' \cdot \nabla \phi_2) dl' \\ \approx \begin{cases} \frac{1}{2} - \frac{D_n \Delta x_n}{4\pi R_c}, & m = n \\ -(\hat{n}_n \cdot \hat{R}) \frac{jk_2}{4} H_1^{(2)}(k_2 |\bar{\rho}_m - \bar{\rho}_n|) D_n \Delta x, & m \neq n \end{cases} \quad (12)$$

$$Z_{mn}^{22} = j\omega\mu_0 \int_{\Delta l_n} \phi_2 dl' \\ \approx j\omega\mu_0 \begin{cases} -\frac{j}{4} \left( 1 - \frac{2j}{\pi} \ln \frac{\gamma k_2 D_n \Delta x}{4e} \right), & m = n \\ -\frac{j}{4} H_0^{(2)}(k_2 |\bar{\rho}_m - \bar{\rho}_n|) D_n \Delta x, & m \neq n \end{cases} \quad (13)$$

Note that in (10) and (12), the second term for  $m = n$  is negligible and can be ignored in the numerical computation. Furthermore, if a linear approximation of the surface contour is used, this term is exactly zero. The elements of the source vector can be written as

$$\bar{E}_m^i = -\hat{y} e^{jk_1(x_m \sin \theta + z_m \cos \theta)} \quad (14)$$

After the unknown current densities and surface fields are solved from the matrix equation, the scattered field can be evaluated by

$$E_y^s = \int_c [j\omega\mu_0 \phi_1 J_y + E_y(\hat{n}' \cdot \nabla \phi_1)] dl' \quad (15)$$

In microwave remote sensing applications, the scattering coefficient is usually the parameter used to represent the scattering characteristics of extensive surface targets. To obtain the scattering coefficient, the far zone scattered field is required which can be obtained by substituting the following far zone approximation of Hankel functions in (15),

$$\phi_1 \approx -\frac{j}{4} H_0^{(2)}(k_1 \rho - k_1 \hat{n}_s \cdot \vec{\rho}') \approx \frac{-je^{j\frac{\pi}{4}}}{\sqrt{8\pi k_1 \rho}} e^{-jk_1 \rho} e^{jk_1 \hat{n}_s \cdot \vec{\rho}'} \quad (16)$$

and

$$\nabla \phi_1 \approx \hat{n}_s \frac{jk_1}{4} H_1^{(2)}(k_1 \rho - k_1 \hat{n}_s \cdot \vec{\rho}') \approx \hat{n}_s \frac{(-k_1)e^{j\frac{\pi}{4}}}{\sqrt{8\pi k_1 \rho}} e^{-jk_1 \rho} e^{jk_1 \hat{n}_s \cdot \vec{\rho}'} \quad (17)$$

where  $\hat{n}_s$  is the unit vector indicating the scattered direction. The far zone scattered field can now be written as

$$\begin{aligned} \text{Icon } \eta_y^s &= \frac{k_1 e^{j\frac{\pi}{4}}}{\sqrt{8\pi k_1 \rho}} e^{-jk_1 \rho} \int_c [\eta J_y - (\hat{n}' \cdot \hat{n}_s) E_y] e^{jk_1 \hat{n}_s \cdot \vec{\rho}'} D dx' \\ &\approx \frac{k_1 e^{j\frac{\pi}{4}}}{\sqrt{8\pi k_1 \rho}} e^{-jk_1 \rho} \sum_{i=1}^N [\eta J_i - (\hat{n}_i \cdot \hat{n}_s) E_i] e^{jk_1 \hat{n}_s \cdot \vec{\rho}'} \sqrt{1 + \left(\frac{\partial z}{\partial x}\right)^2} \Delta x \quad (18) \end{aligned}$$

Note  $\vec{\rho}' = \hat{x}x_i + \hat{z}z(x_i)$ .

The non-coherent scattering coefficient is defined by

$$\sigma^0 = \frac{2\pi\rho}{NL_{eff}} \left[ \sum_{i=1}^{N_s} |E_i^s|^2 - \frac{1}{N} \left| \sum_{i=1}^{N_s} E_i^s \right|^2 \right] \quad (19)$$

where  $L_{eff}$  is the effective illumination length of the antenna pattern. For a Gaussian pattern of the form

$$G(x_i - x_{cen}) = e^{-(x_i - x_{cen})^2 \cos^2 \theta/g^2} \quad (20)$$

The effective illuminating length  $L_{eff}$  can be rewritten as

$$L_{eff} = \int_{-\infty}^{\infty} e^{-2x^2 \cos^2 \theta/g^2} dx = \frac{g\sqrt{\pi/2}}{\cos \theta} \quad (21)$$

### VV polarization

From the scattering geometry in Fig. 1, the vertically polarized incident fields are

$$\bar{E}^i = (\hat{x} \cos \theta - \hat{z} \sin \theta) \eta e^{jk_1(x \sin \theta + z \cos \theta)} \quad (22a)$$

$$\bar{H}^i = -\hat{y} e^{jk_1(x \sin \theta + z \cos \theta)} \quad (22b)$$

Following the same procedure given for the HH polarization, the governing surface integral equations for VV polarization can also be written as

$$H_y^i = \frac{1}{2} H_y + \int_c [j\omega \epsilon_1 \phi_1 K_y + H_y(\hat{n}' \cdot \nabla \phi_1)] dl' \quad (23a)$$

$$0 = \frac{1}{2} H_y - \int_c [j\omega \epsilon_2 \phi_2 K_y + H_y(\hat{n}' \cdot \nabla \phi_2)] dl' \quad (23b)$$

After employing the method of moments, (23) can be simplified to a matrix equation similar to (9). The only differences are that  $E_y$ ,  $E_y^i$  in (9) are replaced by  $H_y$  and  $H_y^i$  and the electric surface current density  $J_y$  is replaced by magnetic current density  $K_y$ . The elements of the matrix have expressions similar to the HH polarization except for the following minor changes.

1. In the expression of  $Z_{mn}^{12}$ ,  $\mu_0$  in HH polarization is replaced by  $\epsilon_1$  for VV polarization
2. In the expression of  $Z_{mn}^{22}$ ,  $\mu_0$  in HH polarization is replaced by  $\epsilon_2$  for VV polarization

After the unknown surface field and surface current density are solved, the scattered field can be evaluated by the following surface integral

$$H_y^s = \int_c [j\omega\epsilon_1\phi_1 K_y + H_y(\hat{n}' \cdot \nabla\phi_1)] dl' \quad (24)$$

In the far zone, the scattered field can be simplified to

$$H_y^s = \frac{k_1 e^{j\frac{\pi}{4}}}{\sqrt{8\pi k_1 \rho}} e^{-jk_1 \rho} \int_c \left[ \frac{K_y}{\eta_1} - (\hat{n}' \cdot \hat{n}_s) H_y \right] e^{-jk_1 \hat{n}_s \cdot \hat{r}'} D dx' \quad (25)$$

The VV polarized scattering coefficient can now be calculated by

$$\sigma_{vv}^0 = \frac{2\pi\rho}{NL_{eff}} \left[ \sum_{i=1}^{N_s} |H_i^s|^2 - \frac{1}{N} \left| \sum_{i=1}^{N_s} H_i^s \right|^2 \right] \quad (26)$$

In the above simulation algorithm, the sampling rate of the surface points is arbitrarily set at eight intervals/simulation unit. To guarantee a sufficient sampling rate, the simulation wavelength is never chosen less than one unit such that at least eight samples per wavelength are always satisfied. The antenna pattern in (20) is there to serve as a tapering function such that the contribution from surface illumination beyond the tapering value of  $10^{-5}$  at  $\theta = 60^\circ$  is negligible. The constant  $g$  in (20) is chosen according to this requirement. The choice of the length of each surface sample  $D$  is chosen to be at least eight times the correlation length of the surface. The number of scattered field samples  $N_s$  is chosen to be 75 so that the confidence interval of  $\sigma^0$  is within one dB.

### III. VERIFICATION OF THE ALGORITHM

To examine surface scattering characteristics by the numerical algorithm developed in this paper, validity of the numerical algorithm must be verified first. The verification can be achieved by comparing the theory with simulation for rough surfaces whose roughness conditions meet the assumptions of the theory. The theories that we choose to make comparison with simulation are the series solution under Kirchhoff approximation and the first order small perturbation approximation [4]. For the purpose of validating the simulation algorithm, the computer generated surface is chosen to be Gaussian in both the surface height distribution and the correlation function [9]. For the sake of completeness, the two-dimensional theoretical expression of the backscattering coefficient for Kirchhoff series solution is given as

$$\sigma_{pp}^0 = |\alpha_{pp}|^2 \frac{k_1 L \sqrt{\pi}}{\cos^2 \theta} e^{-4k_1^2 \sigma^2 \cos^2 \theta} \sum_{n=1}^{\infty} \frac{(4k_1^2 \sigma^2 \cos^2 \theta)^n}{\sqrt{n} n!} e^{-k_1^2 L^2 \sin^2 \theta / n} \quad (27)$$

The parameters  $\sigma$ ,  $L$  are the surface height standard deviation and correlation length respectively. A special surface of interest is the superposition of two independent Gaussian correlated surfaces. The correlation of the composite surface constructed in this manner can be written as

$$\rho(\tau) = A e^{-\tau^2/L_1^2} + B e^{-\tau^2/L_2^2}$$

where  $A = \sigma_1^2/\sigma^2$ ,  $B = \sigma_2^2/\sigma^2$ ,  $\sigma^2 = \sigma_1^2 + \sigma_2^2$ ,  $\sigma_1^2$  and  $\sigma_2^2$  are the height variance of component surfaces and  $L_1$  and  $L_2$  are their correlation lengths respectively. For this correlation, the Kirchhoff series solution can be written as

$$\sigma_{\text{pp}}^0 = |\alpha_{\text{pp}}|^2 4\sqrt{\pi} k_1^3 \sigma^2 L \cos^4 \theta e^{-k_1^2 L^2 \sin^2 \theta} \quad (28)$$

where

$$W^{(n)}(k') = \sqrt{\pi} \sum_{m=0}^n (n, m) A^{n-m} B^m \times \frac{(k' L_1)(k' L_2)}{k' \sqrt{(n-m)(k' L_2)^2 + m(k' L_1)^2}} \exp \left( \frac{(k' L_1)^2 (k' L_2)^2 \sin^2 \theta}{(n-m)(k' L_2)^2 + m(k' L_1)^2} \right)$$

Note that in (27) and (28), the subscripts pp stands for the polarization of either HH or VV. The coefficient  $\alpha_{\text{pp}}$  is the Fresnel reflection coefficient for VV and HH polarizations at normal incidence. For first order small perturbation, the backscattering coefficient can be written as

$$\sigma^0 = |\alpha_{\text{pp}}(\theta)|^2 4\sqrt{\pi} k^3 \sigma^2 L \cos^4 \theta e^{-k^2 L^2 \sin^2 \theta} \quad (29)$$

Where the coefficients  $\alpha_{\text{pp}}$  can be written as

$$\alpha_{\text{hh}} = \frac{\cos \theta - \sqrt{\epsilon_r - \sin^2 \theta}}{\cos \theta + \sqrt{\epsilon_r - \sin^2 \theta}}, \quad \alpha_{\text{vv}} = (\epsilon_r - 1) \frac{\sin^2 \theta - \epsilon_r(1 + \sin^2 \theta)}{[\epsilon_r \cos \theta + (\epsilon_r - \sin^2 \theta)^{1/2}]^2}$$

The conditions of validity for the Kirchhoff approximation are given by [4]

- (1)  $k_1 L > 6$
- (2)  $L^2 > 2.76\sigma\lambda$ , with  $\lambda$  the wavelength incidence.

The conditions of validity for first order small perturbation are

- (1)  $k_1 \sigma < 0.3$
- (2) rms slope,  $\sqrt{2} \sigma/L < 0.3$

A Gaussian correlated surface with roughness parameters  $\sigma = 0.6$  units and  $L = 4.0$  units is chosen for the comparison of simulation with theory. The incident wave length  $\lambda$  is 3 units, with which the values of  $k\sigma$  and  $kL$  are 1.256 and 8.38 respectively. It is noted that for this surface at the wavelength chosen, the Kirchhoff approximation criteria are satisfied. In Figs. 2(a) through 2(c), we have plotted the simulation results along with the Kirchhoff series solution for three values of dielectric constant  $\epsilon_r = 4, 16$  and  $80$ . It is seen that the theoretical results are in good agreement with the simulation for all three dielectric values. By changing the wavelength  $\lambda$  to 14.0 units, the values of  $k\sigma$  and  $kL$  change to 0.269 and 1.795 respectively. It should be noted that for this set of parameters the conditions of validity of first order small perturbation are satisfied. Comparison of the backscattering coefficient between theory and simulation were also performed for three values of dielectric constant. The results are plotted in Figs. 3(a) through 3(c), and excellent agreement between theory and simulation can be observed. The validity of the simulation algorithm is thus confirmed.

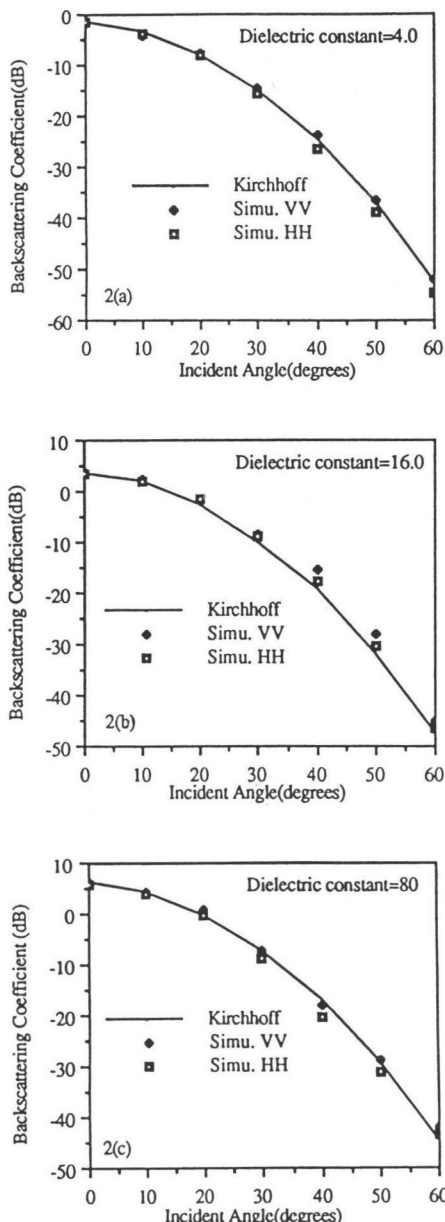


**Figure 2.** Comparison of the backscattering coefficient between simulation and Kirchhoff series solution for Gaussian surface with height standard deviation  $\sigma = 0.6$  units, correlation length  $L = 4$  units, wavelength  $\lambda = 3$  units for (a)  $\epsilon_r = 4.0$ , (b)  $\epsilon_r = 16.0$ , and (c)  $\epsilon_r = 80.0$ .

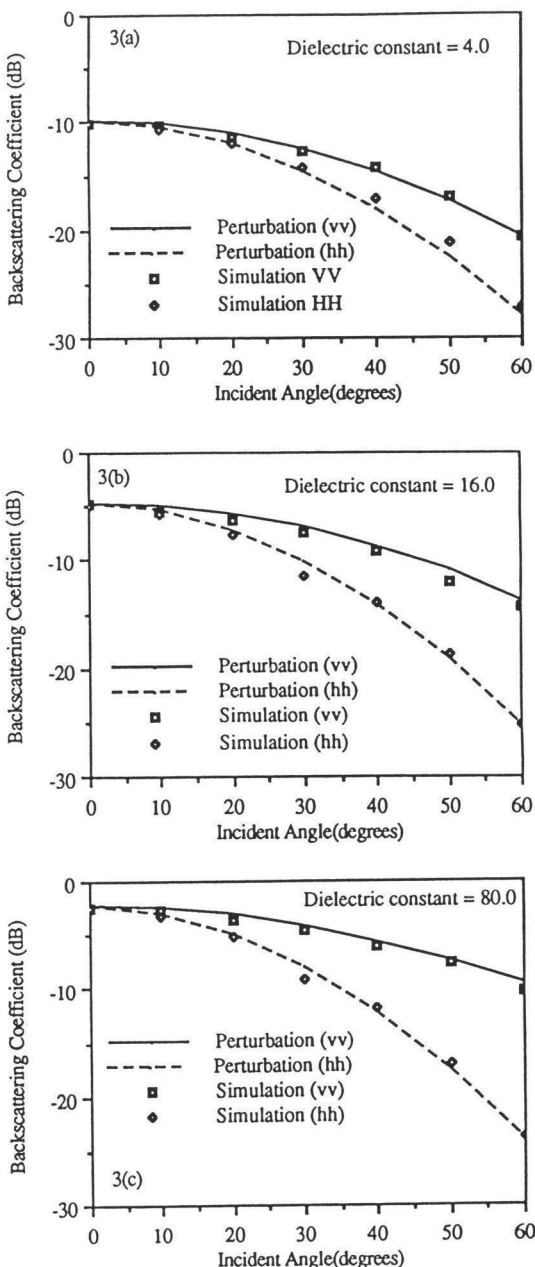


**Figure 3.** Comparison of the backscattering coefficient between simulation and first order small perturbation for Gaussian surface with height standard deviation  $\sigma = 0.6$  units, correlation length  $L = 4$  units, wavelength  $\lambda = 14$  units for (a)  $\epsilon_r = 4.0$ , (b)  $\epsilon_r = 16.0$  and (c)  $\epsilon_r = 80.0$ .

**IV. RESULTS AND DISCUSSION**

In this section we seek to study the scattering characteristics as a function of frequency for both Gaussian and composite surfaces using the developed simulation algorithm. Scattering simulations from the same surface used in Figs. 2 and 3 are performed with incident wave lengths varied from 3 units to 14.0 units and the results are plotted in Fig. 4. In Fig. 4(a), at  $\lambda = 3$  units, surface conditions allow the Kirchhoff approximation to be valid. Good agreement between the Kirchhoff series solution and simulation is observed. Along with the Kirchhoff solution, the first order small perturbation solution is also plotted in Fig. 4(a); as can be seen it is far from the simulation results. Note that under the Kirchhoff approximation, the polarization separation between VV and HH is minimal. This effect is also clearly demonstrated in Fig. 4(a). By increasing the wavelength to 6.0 and 10.0 units as plotted in Fig. 4(b) and 4(c), the difference between VV and HH polarization becomes more and more pronounced and the overall angular trend slows down as compared to the angular trend at higher frequency. This trend continues until the surface and frequency conditions satisfy the first order small perturbation approximation where Bragg scattering is dominant. This phenomenon is plotted in Fig. 4(d) with incident wavelength  $\lambda = 14.0$  units. Note that in Figs. 4(a) through 4(d), corresponding Kirchhoff series solutions are also plotted, and it is seen that the Kirchhoff series solution always lies in between VV and HH polarizations. Similar calculations are also performed for the same surface with dielectric constant  $\epsilon_r$  increased to 80 from 16.0 used in Fig. 4. The results are plotted in Fig. 5(a) through 5(d). Comparison of the two sets of figures indicates that the effect of increasing dielectric constant is to increase the level of the returned signal and the polarization separation between VV and HH; there is very little effect on the angular trend.

One practical case of rough surface scattering is the scattering from the ocean surface. Typically, the ocean surface is composed of two distinctive roughness scales. One scale corresponds to the gravity wave and the other to the capillary wave. The simulation of wave scattering from such large areas as the ocean surface is not yet practical on the computer. However, a scaled down simulation of random surfaces with similar characteristics to that of the ocean can be efficiently simulated. A random surface was constructed by superimposing two Gaussian correlated random surfaces with correlation length  $L$  equals to 4 and 0.5 units respectively. The corresponding surface height standard deviation for the large scale is chosen to be 0.4 units and 0.05 units for the small scale. Simulations are performed for this composite surface with wavelength varying from 1.0 units to 10.0 units. The results for surface with dielectric constant  $\epsilon_r$  of 16.0 are plotted in Figs. 6(a) through 6(d). In Fig. 6(a), where  $\lambda$  is 1.0 unit, it is seen that Bragg scattering does not happen at large angles. This is due to the lack of the small scale that causes Bragg scattering. Although the value of  $k\sigma$  for the small scale is 0.314 which may appear to satisfy the condition of first order small perturbation, the requirement of  $kL$  must also be small is violated [15]. As a result, the prominent polarization separation of VV and HH is not seen at large

angles. The results of the Kirchhoff series solution for the composite correlation along with the Kirchhoff series solution for the large and small scale are also plotted in Fig. 6(a). It is seen that the simulation follows very closely to the Kirchhoff series solution when the composite correlation is used. It is also seen that the result of the composite correlation is the superposition of large and small scale results. This indicates that at this wavelength, both scales can be modeled by the Kirchhoff approximation. The large scale is dominant at small angle of incidence while the small scale is dominant at large angles.

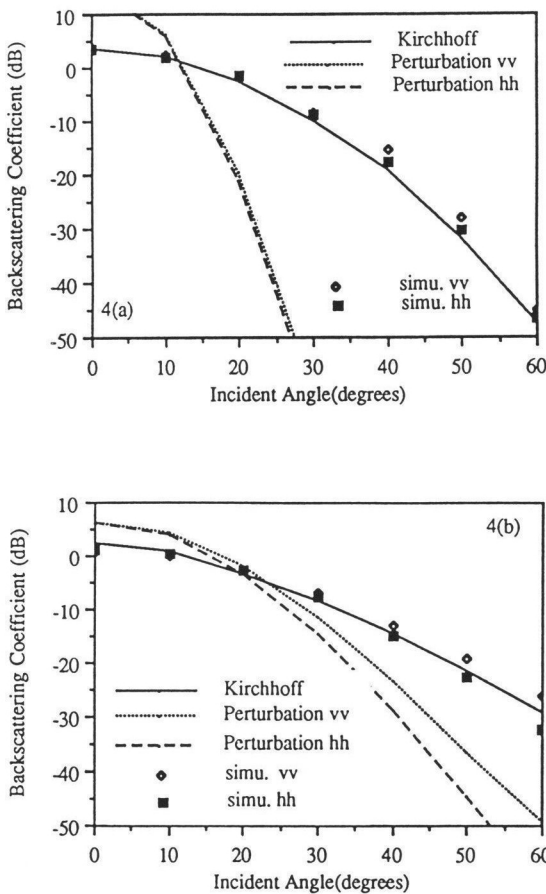


**Figure 4.** The effect of frequency on the backscattering coefficient for Gaussian surface with height standard deviation  $\sigma = 0.6$  units, correlation length  $L = 4$  units, dielectric constant  $\epsilon_r = 16.0$  for (a)  $\lambda = 3$  units,  $k\sigma = 1.257$ ,  $kL = 8.38$ , (b)  $\lambda = 6$  units,  $k\sigma = 0.628$ ,  $kL = 4.188$ , (c)  $\lambda = 10$  units,  $k\sigma = 0.377$ ,  $kL = 2.513$ , (d)  $\lambda = 14$  units,  $k\sigma = 0.269$ ,  $kL = 1.795$ .

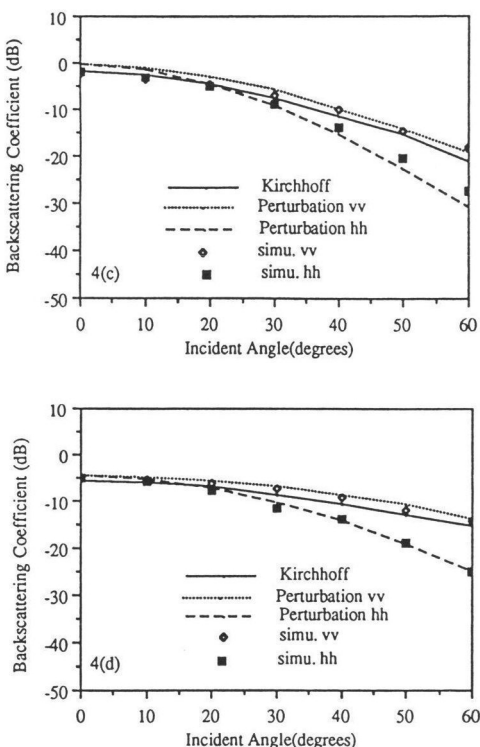


**Figure 4.** Continued.

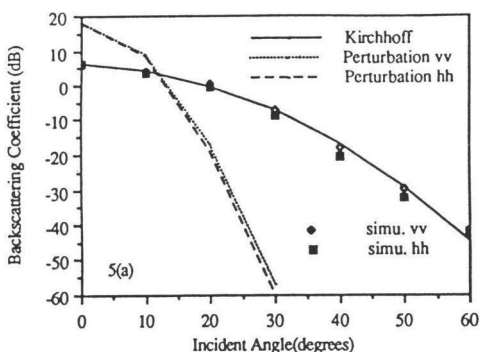


**Figure 5.** The effect of frequency on the backscattering coefficient for Gaussian surface with height standard deviation  $\sigma = 0.6$  units, correlation length  $L = 4$  units, dielectric constant  $\epsilon_r = 80.0$  for (a)  $\lambda = 3$  units,  $k\sigma = 1.257$ ,  $kL = 8.38$ , (b)  $\lambda = 6$  units,  $k\sigma = 0.628$ ,  $kL = 4.188$ , (c)  $\lambda = 10$  units,  $k\sigma = 0.377$ ,  $kL = 2.513$ , (d)  $\lambda = 14$  units,  $k\sigma = 0.269$ ,  $kL = 1.795$ .

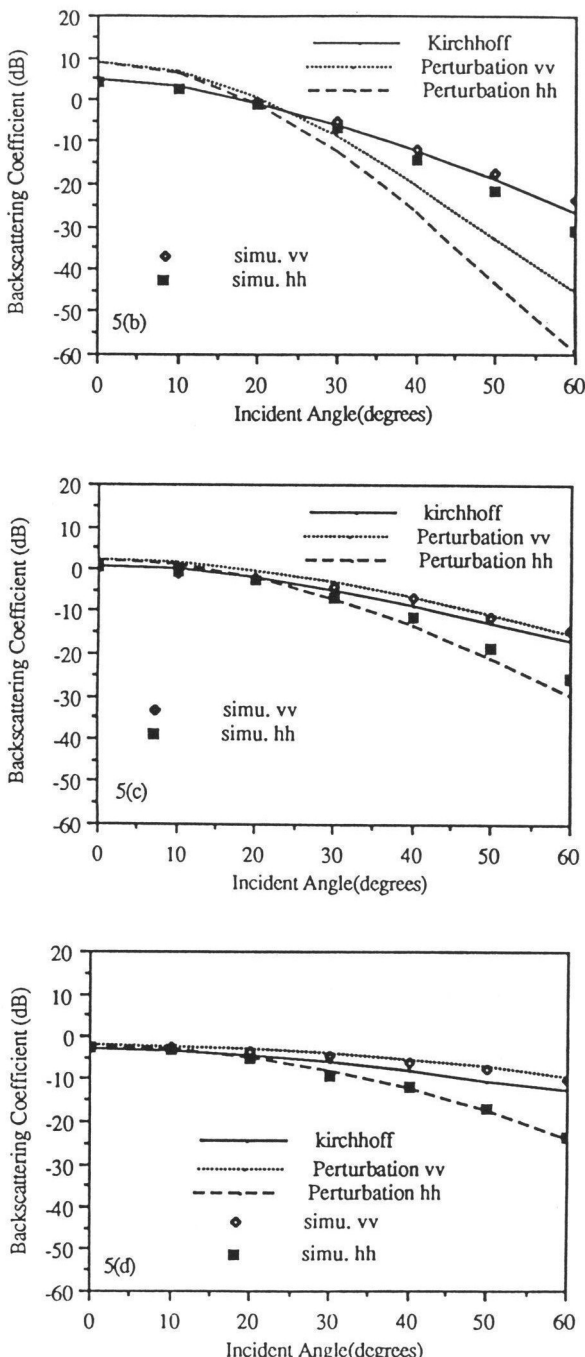
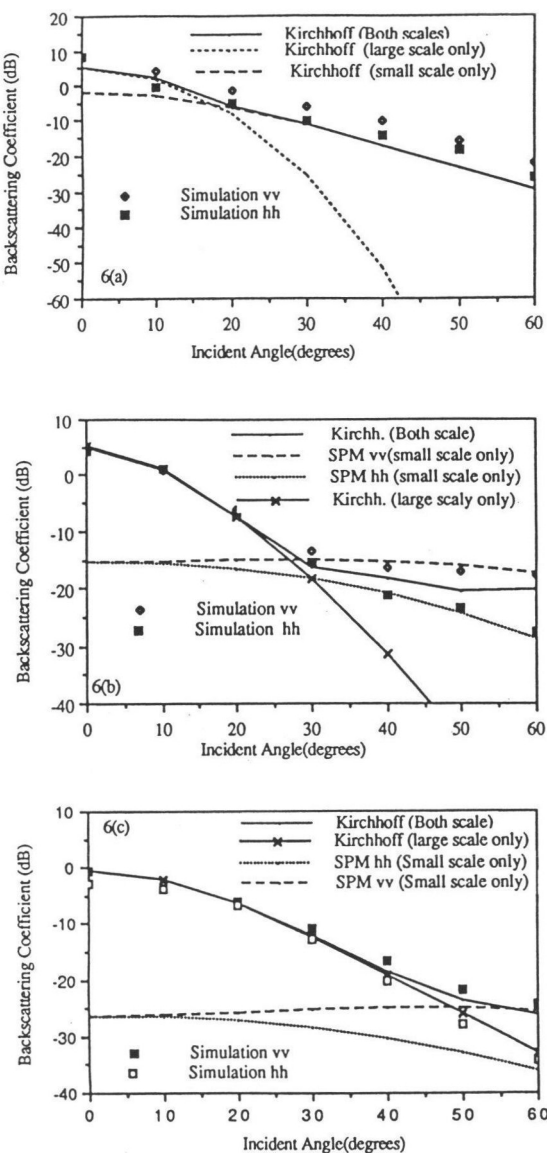


Figure 5. Continued.



**Figure 6.** The effect of frequency on the backscattering coefficient for composite surface with  $\sigma_1 = 0.4$  units,  $L_1 = 4$  units and  $\sigma_2 = 0.05$  units,  $L_2 = 0.5$  units, dielectric constant  $\epsilon_r = 16.0$  for (a)  $\lambda = 1$  unit,  $k\sigma_1 = 2.513$ ,  $kL_1 = 25.13$ ,  $k\sigma_2 = 0.314$ ,  $kL_2 = 3.14$ , (b)  $\lambda = 3$  units,  $k\sigma_1 = 0.837$ ,  $kL_1 = 8.377$ ,  $k\sigma_2 = 0.104$ ,  $kL_2 = 1.04$ , (c)  $\lambda = 7$  units,  $k\sigma_1 = 0.359$ ,  $kL_1 = 3.59$ ,  $k\sigma_2 = 0.0448$ ,  $kL_2 = 0.448$ , (d)  $\lambda = 10$  units,  $k\sigma_1 = 0.251$ ,  $kL_1 = 2.513$ ,  $k\sigma_2 = 0.0314$ ,  $kL_2 = 0.314$ .

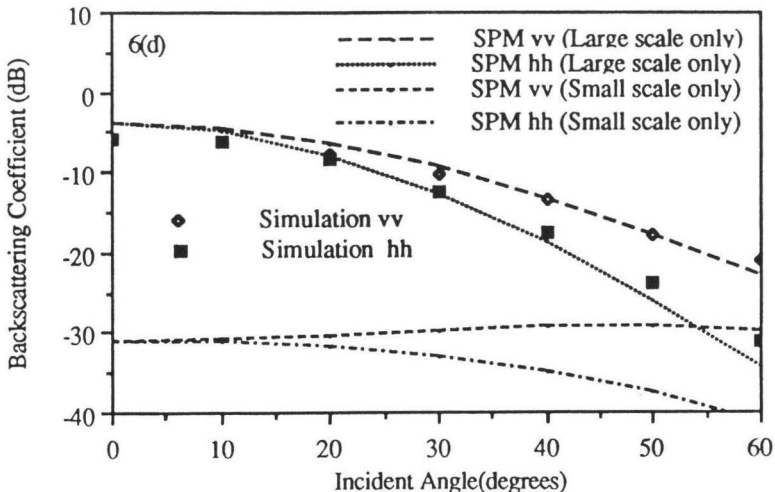
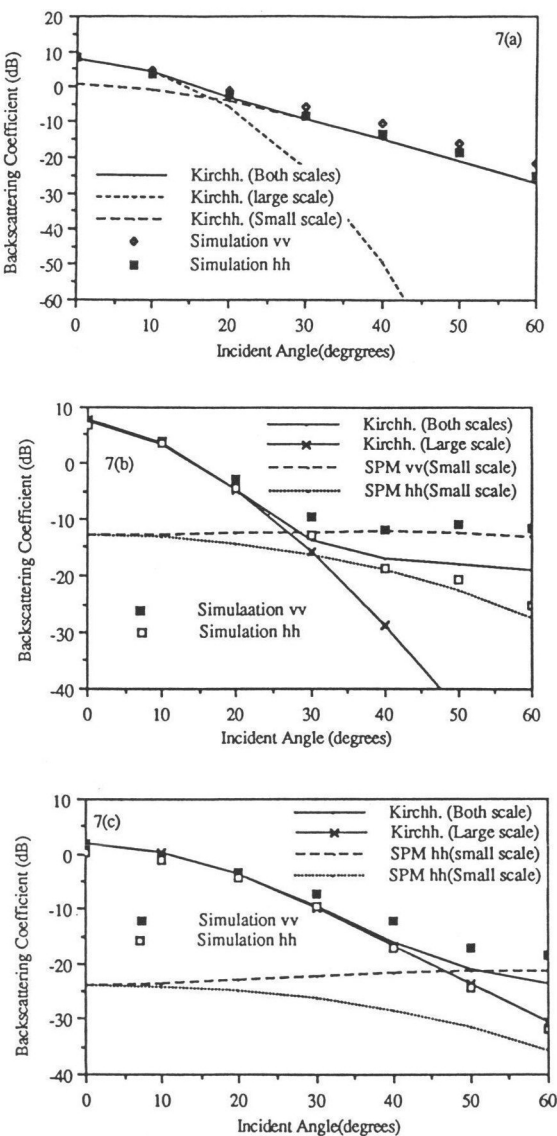


Figure 6. Continued.

When the wavelength increases further to 3 units, as shown in Fig. 6(b), the effect of Bragg scattering becomes dominant at large angles due to the small scale, while the Kirchhoff approximation is dominant at small angles of incidence due to the large scale. This phenomenon is typical for the scattering of the ocean and can be seen by the Kirchhoff series solution of the large scale and the small perturbation solution of the small scale plotted in the same figure. In Fig. 6(b), the result of the Kirchhoff series solution with the composite correlation function is also plotted. It is noted that although the Kirchhoff solution does not distinguish between VV and HH polarizations, decent estimates can still be obtained. When the wavelength increases to 7 units, as shown in Fig. 6(c), the angular range of dominance of the large scale becomes wider while the dominance of small scale is pushed further to large angles. This can be seen by the curves of the Kirchhoff solution of the large scale and the small perturbation solution of the small scale, plotted in Fig. 6(c). Again the Kirchhoff series solution with composite correlation gives fairly good estimates. As wavelength increases further, both the large and small scale satisfy the small perturbation conditions and Bragg scattering is the dominant scattering mechanism at all angles. Since the amplitude of the small scale scattering is insignificant compared to the large scale, the simulation result is expected to agree with the small perturbation solution of the large scale alone. To demonstrate the effect of the dielectric constant, similar simulations were also performed with  $\epsilon_r = 80.0$ . The results are plotted in Figs. 7(a) through 7(d). Again, the effect of dielectric constant is to change the level and the separation of VV and HH polarizations.



**Figure 7.** The effect of frequency on the backscattering coefficient for composite surface with  $\sigma_1 = 0.4$  units,  $L_1 = 4$  units and  $\sigma_2 = 0.05$  units,  $L_2 = 0.5$  units, dielectric constant  $\epsilon_r = 80.0$  for (a)  $\lambda = 1$  unit,  $k\sigma_1 = 2.513$ ,  $kL_1 = 25.13$ ,  $k\sigma_2 = 0.314$ ,  $kL_2 = 3.14$ , (b)  $\lambda = 3$  units,  $k\sigma_1 = 0.837$ ,  $kL_1 = 8.377$ ,  $k\sigma_2 = 0.104$ ,  $kL_2 = 1.04$ , (c)  $\lambda = 7$  units,  $k\sigma_1 = 0.359$ ,  $kL_1 = 3.59$ ,  $k\sigma_2 = 0.0448$ ,  $kL_2 = 0.448$ , (d)  $\lambda = 10$  units,  $k\sigma_1 = 0.251$ ,  $kL_1 = 2.513$ ,  $k\sigma_2 = 0.0314$ ,  $kL_2 = 0.314$ .

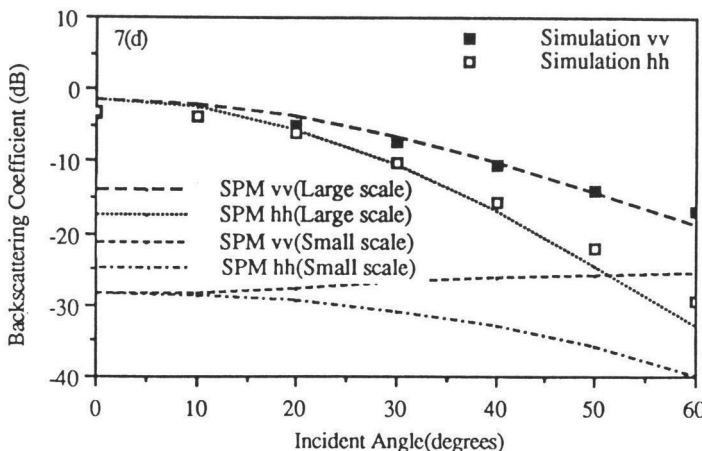


Figure 7. Continued.

## V. CONCLUSIONS

In this paper we have developed the numerical algorithm using the method of moments to simulate electromagnetic wave scattering from dielectric random surfaces. The algorithm was confirmed by comparing simulation with theory at the valid regions of the theories. Beyond the region of validity of theories, numerical simulation is demonstrated in this paper to be a useful and economical tool to study the phenomenon of rough surface scattering.

It is found that for a single scale surface, the effect of increasing frequency on the backscattering coefficient is to gradually diminish the VV and HH polarization separation from that of small perturbation to the Kirchhoff approximation. The angular trend also becomes steeper as frequency increases. For surfaces with distinctively different roughness scales, the frequency behavior of the backscattering coefficient depends on the dominance of the two scales at their respective angular range, i.e., large scale always dominates at smaller angles of incidence while small scale dominates at large angles of incidence. In all cases, the effect of increasing the dielectric constant is to increase the level of backscattering coefficient and the polarization separation between VV and HH.

## ACKNOWLEDGMENTS

This paper is based in part upon work supported by the Texas Advanced Research Program under Grant No. 1861. The computing resources for this work are provided by the University of Texas System Center for High Performance Computing.

The Editor thanks A. Ishimaru, A. A. Maradudin, E. I. Thorsos, and S. C. Wu for reviewing the paper.

**REFERENCES**

1. Isakovich, M. A., "Wave scattering from a statistically rough surface," *Zh. Eksp. Teor. Fiz.*, Vol. 23, No. 3, 305-314, 1952.
2. Brekhovskikh, L. M., "The diffraction of waves by a rough surface, part I," *Zh. Eksp. Teor. Fiz.*, Vol. 5, 275-288, 1952.
3. Rice, S. O., "Reflection of electromagnetic waves from slightly rough surfaces," *Comm. Pure Appl. Math.*, Vol. 4, No. 2/3, 361-378, 1951.
4. Ulaby, F. T., R. K. Moore and A. K. Fung, *Microwave Remote Sensing Active and Passive*, Vol. 2, Addison-Wesley, Reading Massachusetts, 1982.
5. Beckmann, P., and Spizzichino, *The Scattering of Electromagnetic Waves from Rough Surfaces*, Pergamon, New York, 1963.
6. Fung, A. K., and G. W. Pan, "A scattering model for perfectly conducting random surfaces, I. Model development," *Int. J. Rem. Sensing*, Vol. 8, No. 11, 1579-1593, 1987.
7. Winebrenner, D. P., and A. Ishimaru, "Application of the phase-perturbation technique to randomly rough surfaces," *J. Opt. Soc. Am.*, Vol. 2, No. 12, 2285-2293, 1985.
8. Axline, R. M., and A. K. Fung, "Numerical computation of scattering from a perfectly conducting random surface," *IEEE Trans. Antennas Propagat.*, Vol. AP-26, 482-488, 1978.
9. Fung, A. K., and M. F. Chen, "Numerical simulation of scattering from simple and composite random surfaces," *J. Opt. Soc. Am.*, Vol. 2, 2274-2284, 1985.
10. Wu, S. C., M. F. Chen, and A. K. Fung, "Non-Gaussian surface generation," *IEEE Trans. Geosic. Remote Sensing*, Vol. 26, No. 6, 885-888, 1988.
11. Wu, S. C., M. F. Chen and A. K. Fung, "Scattering from non-Gaussian randomly rough surfaces- cylindrical case," *IEEE Trans. Geosic. Remote Sensing*, Vol. 26, No. 6, 790-798, 1988.
12. Thorsos, E. I., "The validity of the Kirchhoff approximation for rough surface scattering using a Gaussian roughness spectrum," *J. Acoust. Soc. Am.*, Vol. 83, No. 1, 78-92, 1988.
13. Thorsos, E. I., "An examination of the full wave method for rough surface scattering," presented at National Radio Science Meeting, University of Colorado, Boulder, Colorado, January 1988.
14. Poggio, A. J., and E. K. Miller, "Integral equation solution of three-dimensional scattering problems," *Computer Techniques for Electromagnetics*, (Chapter 4), Pergamon, New York, 1973.
15. Chen, M. F., and A. K. Fung, "A numerical study of the regions of validity of the Kirchhoff and small perturbation rough surface scattering models," *Radio Science*, Vol. 23, No. 2, 163-170, 1988.

M. F. Chen received the B.S. degree in geology from Cheng Kung University, Taiwan, in 1973 and the M.S. and Ph.D. degrees in electrical engineering from the University of Kansas, Lawrence, Kansas in 1981 and 1984. From 1984 to 1985, he was with the Wave Scattering Research Center of the University of Texas at Arlington as a post doctoral fellow. From 1985 to 1986, he was with the Electrical Engineering Department of the University of Texas at Arlington as a visiting assistant professor. In 1987, he joined the department as an assistant professor. His current research interests are in the area of modeling and numerical simulation of wave scattering from random surfaces, random media and their applications to Remote Sensing.

**Shu-Yui Bai** was born in Chang Hua, Taiwan, Republic of China on October 8, 1961. She received her B.S. degree in physics science in 1985 from the National Tsing Hua University in Hsinchu, Taiwan and M.S. degree in electrical engineering in 1988 from the University of Texas at Arlington in USA. She then became a member of technical staff of Wave Scattering Research Center in Electrical Engineering Department in the University of Texas at Arlington. Ms. Bai has been an engineer in a PC-board manufacturing company in California since 1989. She has concentrated on design and development of test software and procedure for standard and/or custom electronic devices. She will continue her advanced study in the Ph.D. program in 1990. Her research interests are in theories and applications for microwave remote sensing.